Ti 2p X-ray absorption in titanium dioxides (TiO_2): the influence of the cation site environment

1994 J. Phys.: Condens. Matter 6 10811

(http://iopscience.iop.org/0953-8984/6/49/022)

J. Phys.: Condens. Matter 6 (1994) 10811–10821. Printed in the UK

Ti 2p x-ray absorption in titanium dioxides (TiO_2): the influence of the cation site environment

J P Crocombette and F Jollet

CEA, DSM/DRECAM/SRSIM, Centre d'Etudes de Saclay, Batiment 462, 91191 Gif-sur-Yvette Cédex, France

Received 9 August 1994, in final form 20 September 1994

Abstract. The influence of local order around the titanium site on Ti 2p x-ray absorption spectra is studied for rutile, anatase and brookite. This is done by a configuration interaction based calculation of Ti $L_{2,3}$ x-ray absorption edge shapes, explicitly taking into account the exact first-neighbour surroundings of the cation acting through crystal field splitting and hopping terms. The evolution of the peak splittings and intensities from rutile to anatase is well reproduced for the L_2 edge and can be attributed to the small changes in the cation site symmetry. In contrast the splitting of the second peak of the L_3 edge cannot be attributed to differences in the first coordination shell of the cation between the titanium oxides.

1. Introduction

Due to their technological importance in the field of catalysis as well as for the elaboration of high-T_c superconducting oxides, titanium oxides have been widely studied, especially their chemical and electronic properties [1, 2]. The latter have been experimentally investigated by, among other methods, electron spectroscopies such as direct or inverse x-ray photoelectron spectroscopy [3, 4], x-ray absorption (XAS) [5–7] and electron energy loss spectroscopy (EELS) [7, 8]. As from a structural point of view, the Ti site presents a symmetry more or less the same in several compounds, the authors often had to discuss the importance of short- and long-range order effects to interpret the spectra, especially for the Ti 2p EELS and XAS edges [6, 7]: indeed, on one hand, such a threshold is known to be very sensitive to local order, both because of the 2p core hole–d electron attraction and because of the influence of the crystal field on d orbitals. On the other hand, long-range order interactions, such as the Madelung field, have great importance for the electronic structure of oxides. The knowledge of the relative importance of short-range versus long-range interactions in such materials is therefore a crucial point in the understanding of their electronic structure. From this point of view, the case of the three polymorphs of TiO_2 (rutile, anatase and brookite) is of particular interest, as the Ti site symmetry in these oxides is close to octahedral, so they constitute a fine structure sensitivity test.

The Ti 2p experimental thresholds of rutile and anatase have recently been obtained by EELS [7] and those of rutile, anatase and brookite by XAS [6]. These results show differences between the spectra, which have been interpreted by theoretical calculations: multiple-scattering and band structure calculations are discussed in [7], while a multiplet approach is used in [6]. Another approach based on configuration interaction (CI) calculations for an octahedral surrounding of the cation is presented in [9] for the Ti 2p XAS in $SrTiO_3$. In these papers, the authors show nice calculations for different perfect symmetries (O_h, D_{4h},

0953-8984/94/4910811+11$19.50

D_{3d} in [6]; O_h in [9]). However, in order to discuss local order on Ti distorted octahedral sites in Ti oxides, the approximation of a perfect O_h or D_{4h} symmetry may be questionable.

In this paper, we present CI calculations of the Ti $L_{2,3}$ XAS edge shapes in rutile, anatase and brookite. The interest of our approach is that it deals with any real surroundings of the cation site, which enables us to consider even slight symmetry differences, as encountered in Ti oxides, and to take into account the covalency of the oxides through the hopping terms. Such an approach has already been successfully applied to the case of site selectivity in ZrO_2 doped Y_2O_3 [10]. The paper is organized as follows: section 2 is devoted to the calculation method and to the way the parameters are chosen. In section 3, a comparison with experimental results is made, and the importance of local order to the Ti 2p edge shapes is discussed.

2. Ti 2p edge shape calculations

2.1. *The calculation method*

We consider a cluster made of a central transition metal cation surrounded by its oxygen first neighbours. The ions are in exact positions relative to each other. The 2p orbitals of the O atoms and the d and 2p orbitals of the cation are considered. Configurations with more than one ligand hole have been neglected in our calculations. The Hamiltonian of the system takes into account the charge transfer through hopping terms, the crystal field splitting and the intracationic electronic repulsions (i.e. d electron interactions and electron–core hole interactions). Since the exact O surroundings are provided, it proves possible to calculate the O 2p–cation d and O 2p-O 2p hopping terms for each pair of atoms. Exact positions of O atoms also enable us to calculate the exact crystal field splitting [10]. Assuming an ionic point charge on each O atom, the total crystal field is the sum over all first neighbours of the potential created by each of them. The matrix elements involve two quantities $\overline{r^2}$ and $\overline{r^4}$ formally equal to the mean values of r^2 and r^4 where r is the radial d orbital distribution. As explained in [11], they cannot be properly connected to calculated values of their formal expressions, so they have been treated as parameters in our calculation.

The resulting 5×5 matrix is diagonalized, leading to eigenvalues and eigenvectors of the crystal field. What is obtained at the end is a set of five vectors labelled from $\delta = 1$ to $\delta = 5$, with crystal field energy Δ_δ. These vectors constitute, from now on, the d orbital basis set. It must be stressed here that, within this approach, only the two parameters $\overline{r^2}$ and $\overline{r^4}$ are necessary to obtain the eigenvalues and eigenvectors of the crystal field, whatever the local order around the cation may be. O 2p orbitals are expressed in the usual p_x, p_y, p_z basis set.

The Hamiltonian of the cluster is written out in the basis of Slater determinants:

$$H = \sum_{2p,2p'} \zeta_{2p2p'} C^+_{2p} C_{2p'} + \sum_{\delta,\sigma} (\epsilon_d + \Delta_\delta) C^+_{\delta\sigma} C_{\delta\sigma} + \sum_{\pi,\sigma} \epsilon_p C^+_{\pi\sigma} C_{\pi\sigma}$$
$$+ \sum_{\pi,\delta,\sigma} (V_{\pi\delta} C^+_{\delta\sigma} C_{\pi\sigma} + V^*_{\pi\delta} C^+_{\pi\sigma} C_{\delta\sigma}) + \sum_{\pi,\pi',\sigma} V_{\pi\pi'} C^+_{\pi'\sigma} C_{\pi\sigma}$$
$$+ \sum_{\substack{\nu_1,\nu_2,\nu_3,\nu_4 \\ \sigma,\sigma'}} U_{\nu_4\nu_3\nu_2\nu_1} C^+_{\nu_4\sigma} C^+_{\nu_3\sigma'} C_{\nu_2\sigma'} C_{\nu_1\sigma}$$

where 2p runs over metal 2p spinorbitals, δ runs over the d orbitals, π over the O 2p orbitals, ν over all metal orbitals and σ over the spins, up or down.

$\zeta_{2p2p'}$ are the spin–orbit coupling matrix elements of the cation 2p orbitals. ϵ_d and ϵ_p are the atomic energies of cation d and O 2p orbitals, respectively. Δ_δ is the crystal field energy of the δ orbital.

$V_{\pi\delta}$ and $V_{\pi\pi'}$ are the hopping matrix elements, calculated by Slater–Koster equations [12], which take into account the relative geometry of orbitals. The radial dependences of these terms are calculated by Harrison's formulae [13], which involve two parameters η_σ and η_π measuring the amount of σ and π bonding, respectively. We fixed the usual ratio $\eta_\pi = -0.5\eta_\sigma$.

$U_{\nu_4\nu_3\nu_2\nu_1}$ are the intracationic electronic repulsions expressed in terms of Slater integrals F^0_{dd}, F^2_{dd}, F^4_{dd}, F^0_{pd}, F^2_{pd}, G^1_{pd} and G^3_{pd} [14]. The spin–orbit coupling of d orbitals was neglected in our calculations.

The 2p XAS spectrum is dominated by dipole allowed transitions to d and s final states. Due to larger wavefunction overlap the d channel is much stronger than the s one. Subsequently the latter is neglected. According to the Fermi golden rule, the absorption cross-section is given by

$$\sigma(E) \propto \sum_F |\langle\Phi_G|\varepsilon \cdot r|\Phi_F\rangle|^2 \delta(E_G + h_\nu - E_F)$$

where F runs over the final states.

The ground state of the cluster is first calculated. The dipolar operator $\varepsilon \cdot r$ is then developed in terms of spherical harmonics Y_{1m}, and its matrix elements, constituting the dipole transition probabilities from 2p core states to d orbitals, are calculated. Projection on the final states gives the theoretical spectrum.

Core hole intrinsic lifetime broadenings as tabulated in [15] (i.e. 0.1 eV for L_3 and 0.24 eV for L_2 edges) have been used. A supplementary convolution with a Gaussian broadening ($\sigma = 0.4$ eV) was applied to account for experimental resolution.

2.2. *Parameters*

The parameters used in the calculation to fit the experimental spectra are as follows.

(i) $\overline{r^2}$ and $\overline{r^4}$ for crystal field splittings.

(ii) $\Delta = \varepsilon_d - \varepsilon_p$ and η, which is the multiplicative factor in Harrison's formulae for hopping terms. These two terms pilot the charge transfer from O to cation d orbitals.

(iii) F^0_{pd}, which is the isotropic attraction of the final state 2p core hole for the d electrons. F^0_{dd} was deduced from [16] and kept constant.

The last parameter concerns the other Slater integrals F^2_{dd}, F^4_{dd}, F^2_{pd}, G^1_{pd} and G^3_{pd}, which control the multiplet splitting on the cation. All these integrals have been taken from *ab initio* Hartree–Fock calculations [17], but these values obtained by the monoelectronic method should be reduced to account for intraatomic correlation effects before use in CI calculations [18]. Different coefficients of reduction are used in the literature. We decided to treat this multiplication factor as a free parameters denoted m.

The spectra for the different forms of Ti oxide we considered present globally the same shape and the same variation with regards to the parameters. The figures to support the discussion are for rutile but the discussion itself can apply to any form of Ti oxide. The theoretical spectra present a form close to the one of a formal d^0 in O_h symmetry [9]. Due to 2p spin–orbit coupling they are divided into two sets of peaks forming the L_3 and L_2 edges. Each edge's main feature is the occurence of two peaks directly related to t_{2g} and e_g orbital spittings in perfect O_h symmetry. These peaks can be considered as being t_{2g} like

and e_g like in the particular point group symmetry of rutile (D_{2h}). Focusing on the L_2 edge, two quantities can be defined to characterize the spectral shape: the distance between the main peaks A_2–B_2 and the intensity ratio A_2/B_2 (see figure 1). Equivalent quantities can be defined for the L_3 edge and their variations are the same for both edges.

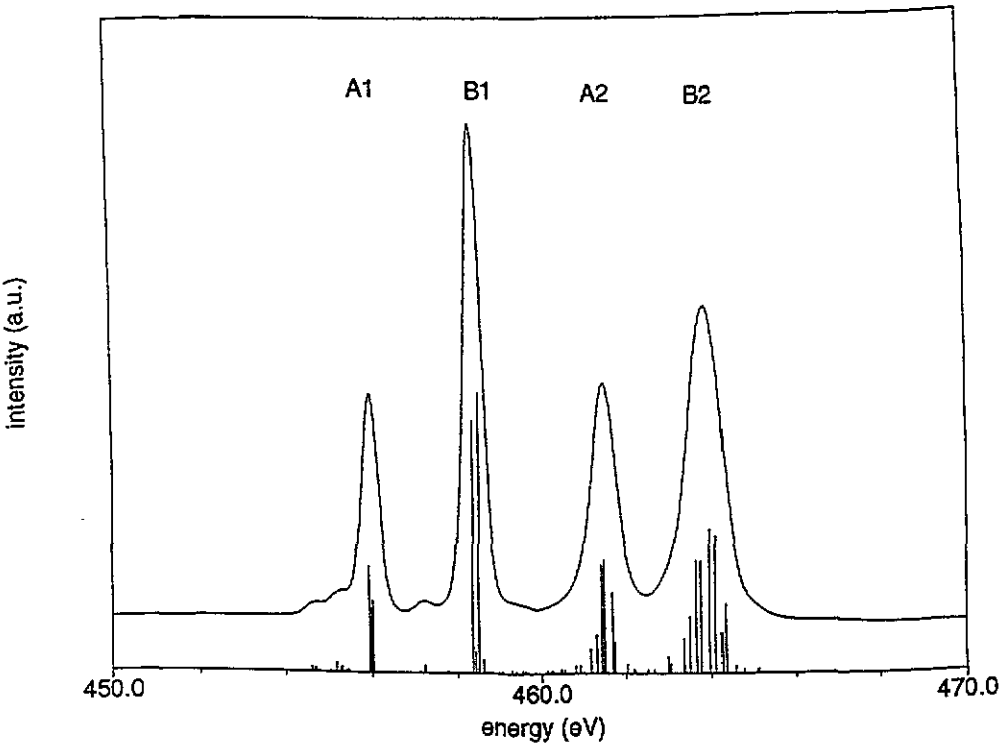

Figure 1. Calculation of the Ti 2p x-ray absorption edge in rutile. The solid line indicates the broadened spectrum; vertical bars are poles of the spectrum.

The effect of the crystal field confirms the study in the ionic limit made in [17]: increasing $\overline{r^2}$ and $\overline{r^4}$ causes an increase in the crystal field splitting, which leads to an increase in the peak separation and in A_2/B_2.

Considering the effect of the multiplication factor for the Slater integrals m, we observed that when m rises (for instance from 50% to 90%) A_2–B_2 increases and A_2/B_2 decreases (see figure 2). To account for these trends it should be noted that m measures the importance of the multiplet core hole–d electron interactions. This multiplet creates the small prepeaks on the low-energy side of the L_3 edge and is responsible for the deviation of A_2/B_2 from the statistical value of $\frac{3}{2}$. Varying m also changes the branching ratio between the L_2 and L_3 parts of the spectra. When m increases, the branching ratio, defined as $I(L_3)/[I(L_2) + I(L_3)]$, decreases. This is due to the rise of Slater integrals with regards to spin–orbit coupling of the 2p core states [19].

Allowing for configuration interaction produces a rise in A_2–B_2 and A_2/B_2. This can be explained from a molecular orbital (MO) point of view. The promoted core electron probes the d part of the empty MO. It is known that when charge transfer is taken into account the separation between the d MO is larger than the only ionic crystal field splitting, this

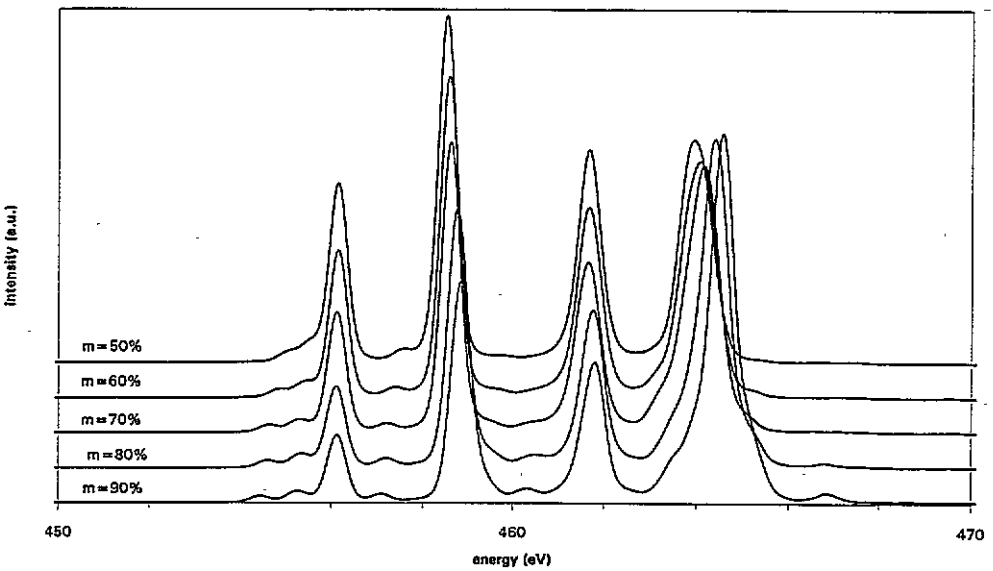

Figure 2. The variation of the Ti 2p x-ray absorption edge with Slater integral reduction coefficient m in rutile.

separation being an ascending function of the charge transfer. The empty MO bears less weight on the atomic d orbitals, lowering the influence of the core hole on them and making A_2/B_2 closer to the statistic value of $\frac{3}{2}$. No systematic study of the spectral shape variation with the charge transfer parameters (Δ, η and F^0_{pd}) was done as they were obtained from a fit of cation 2p x-ray photoelectron spectroscopy (XPS) in rutile. Indeed, our code enables us to simulate cation 2p XAS and also cation 2p XPS. The experimental 2p XPS of rutile presents two peaks due to 2p spin–orbit coupling and two satellites 13.5 eV distant from the main peaks and having an intensity of about 8% of the main ones. Following recent works [20, 4], these satellites are due to charge transfer process in the final state because of the core hole attraction on the d orbitals. We decided to fix our parameters Δ, η and F^0_{pd} (all acting on charge transfer) so as to reproduce the experimental 2p XPS. During this fitting procedure we found the same trends as Parlebas [20] with regard to the variation of the parameters. The other parameters $\overline{r^2}$, $\overline{r^4}$ and m were not considered in the fit as they have, in a first approach, little influence on the spectral XPS shape. The values obtained are given in table 1.

Table 1. A list of the parameters used for the calculation of the $L_{2,3}$ spectra.

2p XPS	$\Delta = 4$ eV	$F^0_{pd} = 8$ eV	$\eta_\sigma = -1.9$
2p XAS	$\overline{r^2} = 0.35$ Å^2	$\overline{r^4} = 1.1$ Å^4	$m = 60\%$

The charge transfer parameters being fixed, we returned to the 2p XAS for which the multiplication factor and crystal field splitting remained to be determined. Fitting rutile spectra, we obtained the values of table 1. With exactly the same set of parameters, we made calculations for TiO_6 clusters in anatase and brookite. The differences between our theoretical spectra originate therefore only from the different positions of the O first neighbours around Ti ions.

3. Discussion

3.1. Experimental results

We briefly recall here some features of the crystallographic structures of the different forms of the Ti oxides we consisder. In these four forms each Ti atoms is coordinated to six O neighbours. In each case the coordination O octahedron is slightly distorted. The site symmetry and bond lengths are given in table 2 (from [6]). As can be seen in figure 3, the rutile octahedron is only slightly distorted, whereas anatase and even more brookite present strong distortions. Nevertheless it is to be stressed that the structures differ more in the secondary coordination shell and in the way the TiO_6 octahedra are joined together. These differences are not considered in this paper, in which we focus on the first-coordination-shell influence.

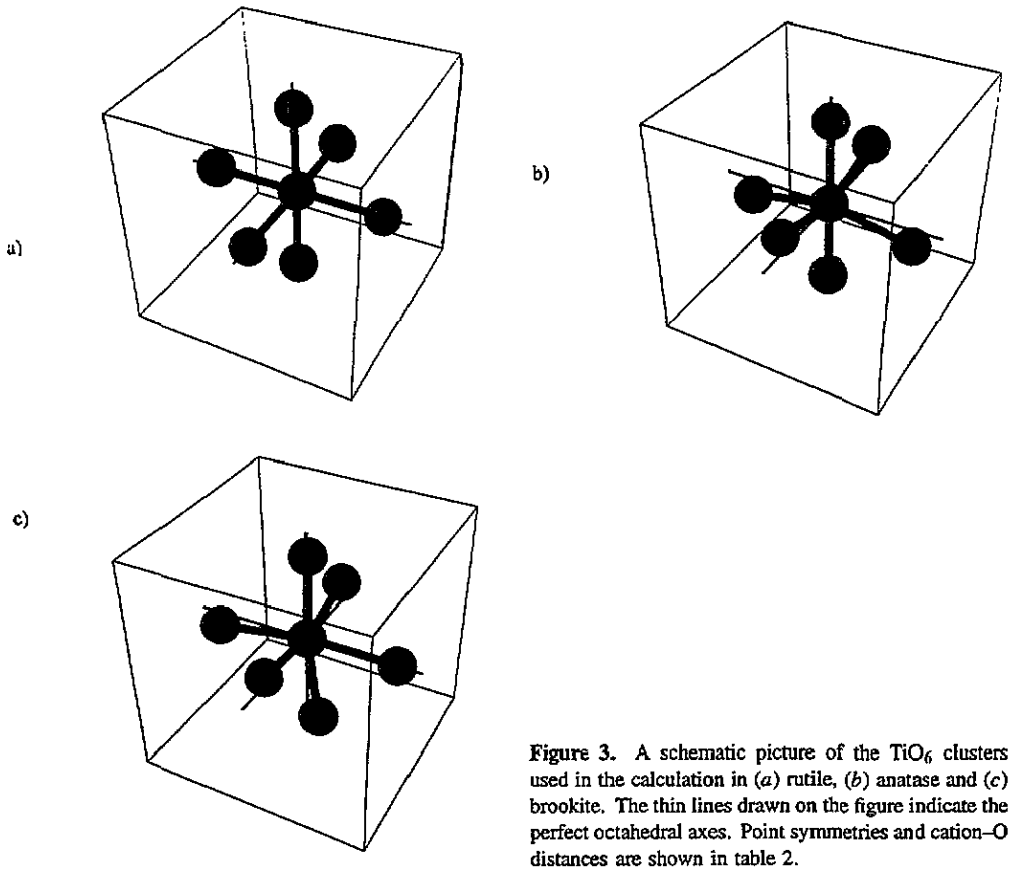

Figure 3. A schematic picture of the TiO_6 clusters used in the calculation in (*a*) rutile, (*b*) anatase and (*c*) brookite. The thin lines drawn on the figure indicate the perfect octahedral axes. Point symmetries and cation–O distances are shown in table 2.

Table 2. Structural parameters of the Ti oxides (from [6]).

Material	Symmetry	Cation–O bond lengths (Å)
Rutile	D_{2h}	1.946 (4), 1.984 (2)
Anatase	D_{2d}	1.937 (4), 1.983 (2)
Brookite	C_1	1.87, 1.92, 1.94, 1.99, 2.00, 2.04

The experimental 2p XAS spectra for rutile, anatase and brookite of [6] are reproduced in figure 4. For rutile and anatase, one can also refer to [7]. These spectra present several differences.

(i) The shapes of the high-energy part of the L_3 edge (peak B_1) are different for the three compounds. They are composed of two peaks producing a low-energy shoulder for rutile, a high-energy one for anatase and a broad peak for brookite.

(ii) The energy separation and intensity ratios as defined in the preceding section, A_2–B_2 and A_2/B_2 vary among the materials (see table 3 and table 4, respectively). The splitting of the L_2 edge grows from 1.97 eV for anatase to 2.45 eV for rutile [7] with the intermediate value of approximately 2.25 eV for brookite. The intensity ratio A_2/B_2 increases with A_2–B_2. For the L_3 edge similar variations exist although they are partially hidden by the division of peak B_1.

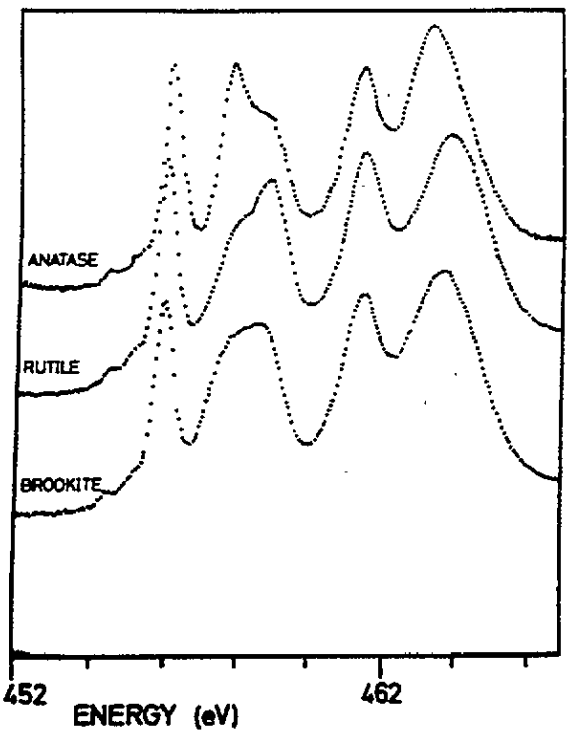

Figure 4. Experimental 2p XAS spectra of rutile, anatase and brookite (from [6]).

Table 3. A_2–B_2 splitting of the L_2 edge in electronvolts.

	Experimental splitting	Theoretical splitting	Crystal field splitting
Rutile	2.45	2.43	1.96
Anatase	1.97	2.10	1.78
Brookite	2.25	2.20	1.79

Table 4. A_2/B_2 intensity ratio for the L_2 edge. The experimental ratios are approximate values deduced from the experimental spectra.

	Experimental ratio (%)	Theoretical ratio (%)
Rutile	88	76
Anatase	77	54
Brookite	81	59

3.2. The influence of the cation site symmetry

Our theoretical spectra are given in figure 5. Apart from the splitting of the peak B_1, which will be considered later, our calculations reproduce well the experimental edges. The small prepeaks that appear in both the calculations and the experiments are related to multiplet splittings of the electron–hole interactions. The values of the splitting A_2–B_2 are well reproduced (see table 3). We stress again that the differences between our results originate only from the differences in the first coordination shell, the parameters being the same for all materials. In particular, we reproduce the increase of A_2–B_2 and A_2/B_2 from anatase to brookite to rutile.

The differences in A_2–B_2 between the materials can be seen in their ionic crystal field splittings. With the parameters of table 1, the d orbitals are split into two sets of nearly degenerate obitals, t_{2g} like and e_g like, but the small differences in the first coordination shell change the value of the energy differences between t_{2g} and e_g like orbitals (see table 3). They are ordered like the A_2–B_2 splittings of the spectra, but are smaller, due to the importance of non-ionicity in spectral shape. It can also be seen that the charge transfer increases the differences between brookite and anatase, which are barely noticeable as far as crystal field is concerned but become significant with the full calculation. This enhancement proves the need to consider charge transfer to reproduce 2p XAS spectra. Charge transfer in the ground state is measured as the total weights of $d^1\underline{L}$ configurations (table 5). They are nearly equal in all materials.

Table 5. Total weights of $d^1\underline{L}$ configurations.

	Percentage of $d^1\underline{L}$
Rutile	37
Anatase	40
Brookite	39

Charge transfer is also very important with regard to A_2/B_2 ratios (see table 4). If it is neglected, the ratios appear in the correct order, ascending from anatase to rutile, but are much smaller than the experimental ones. Allowing for non-ionicity produces a dramatic increase in the first peaks, A_2/B_2 becoming large enough to compare roughly with the experiment.

3.3. The B_1 peak

Our theoretical spectra (figure 5) do not show any division of peak B_1. In the lack of this separation this peak appears too intense in our calculations. Different explanations have been proposed to account for this division. De Groot *et al* [6] propose that the different distortions from O_h symmetry produce different splittings of the e_g peak. Our calculations do not confirm this explanation. In [17], a calculation in D_{4h} site symmetry is presented

to account for Ti 2p XAS in rutile: even if the exact site symmetry of Ti in rutile is D_{2h}, the atomic positions make it very close to D_{4h} and it can be approximated to be D_{4h}. The way the crystal field is handled in [17] allows the authors to find a quite good agreement for the division of peak B_1. Indeed, they consider the crystal field from the point of view of symmetry reduction: the d orbitals are degenerate in spherical symmetry; in O_h symmetry they split in two subsets t_{2g} and e_g, so that one parameter is needed to fit the experimental spectra. When the symmetry is further reduced to D_{4h}, the five d orbitals form four subsets: the crystal field makes the d orbitals have four different eigenenergies. The relative positions of these four peaks are determined by three parameters related to symmetry properties. These three quantities are treated as free parameters in their calculation. Thus they succeed in finding a set of parameters leading to peak positions, which together with the multiplet splitting reproduce the spectra nicely. However, in doing this they focus only on point group properties and forget the actual positions of atoms. As a matter of fact, in the framework of the present point charge crystal field calculations, these three parameters can be related to the amount of distortion from O_h symmetry [21]. The values used in [6] correspond to a ratio between the planar cation–O distance and the axial cation–O distance of 0.76, but in rutile, for which the octahedral site is only slightly distorted, this ratio is 0.98. In contrast, we do consider the surrounding atoms in their actual positions. Atomic positions being fixed, our parameters $\overline{r^2}$ and $\overline{r^4}$ allow us to explore all the possible crystal field splittings. We of course find that, for D_{4h} symmetry, there are four crystal field peaks but neither in rutile nor in anatase or brookite was it possible to find a set of parameters $\overline{r^2}$ and $\overline{r^4}$ that split the peak B_1 satisfactorily. Even if small divisions of the e_g orbitals exist and produce very small divisions of the e_g peaks hidden by broadenings, they can be no means be enlarged enough to reproduce the large division of peak B_1, the reason for this being that a similar division exists for the t_{2g} orbitals and that forcing an important splitting of the e_g orbitals creates also a strong separation of the t_{2g} orbitals so that the spectra can no longer be compared with the experimental spectrum. An attempt to include the crystal field from Ti second neighbours was performed, but this additional crystal field is very low compared to the first-neighbour one, due to the quick decrease of the crystal field as a function of distance between the cation and the surrounding charges, so no improvement was obtained (the crystal field is not to be confused with the Madelung field).

Brydson *et al* [7] propose other explanations. First, they suggest a division of the MO in the e_g band. With respect to this point, our calculations, including only first O neighbours–Ti charge transfer, may indicate that the division would originate from a longer-range effect, at least second-neighbour interactions. The strong differences in Ti second coordination shell could be responsible for the different splittings of B_1. Such a longer-range effect has already been observed in the 2p XPS of nickel and copper oxides [22]. Brydson *et al* [7] alternatively suggest that the splitting may originate from a dynamic Jahn–Teller effect, that is, a coupling of electronic and vibrational states, which would split the e_g orbitals. Such splittings, associated with much smaller splitting of the t_{2g} orbitals are observed, in optical measurements, for Ti octahedrally coordinated compounds [23–25]. Our approach does not allow us to check this point, the atoms being frozen in their positions in the final state, but it should be noted that the observed optical splittings are always small compared to the large division (approximately 1 eV) of peak B_1.

The last point we would like to mention is that it seems to be commonly admitted that this splitting is also present for peak B_2 of the L_2 edge but is blurred by extra broadenings. In view of the experimental spectra, we think that this splitting is smaller for the L_2 edge than for the L_3 one. Maybe the presence and nature of the core hole is to be considered

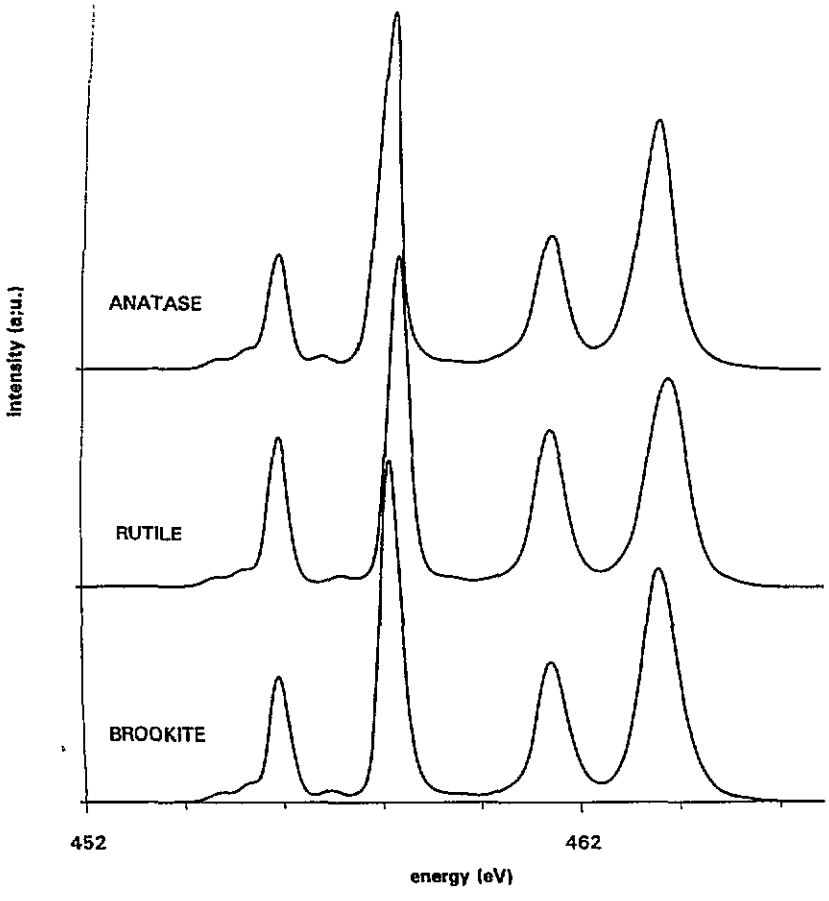

Figure 5. Calculation of the Ti 2p x-ray absorption edge in rutile, anatase and brookite. The same set of parameters was used in the three calculations (see table 1).

to account for this splitting, even if, as we prove, the multiplet interactions alone cannot explain it.

4. Conclusions

We have calculated the Ti 2p x-ray absorption edge of rutile, anatase and brookite by a configuration interaction code able to discriminate the different local environment of the Ti site in these compounds. We confirm that the major features of the spectra are close to the O_h symmetry ones.

We show that the differences in the A_2–B_2 energy separations and in the A_2/B_2 intensities between the spectra can unambigiously be accounted for by the differences in the first coordination shell of the Ti atoms. If crystal field effects are clearly important, it proves also necessary to take into account the non-ionicity to reproduce the spectra satisfactorily.

Even if the total weight of $d^1\underline{L}$ configurations is nearly equal for each material, charge transfer effects produce noticeable differences in the spectra.

We also show that the 2p XAS spectral shape, which is usually thought to be dominated only by local order effects, cannot be entirely explained by local order arguments. Indeed our calculations prove that the distortions from O_h symmetry do not explain the splitting of the second peak of the L_3 edge.

Acknowledgments

Dr F M F de Groot is acknowledged for allowing us to reproduce figure 4. We are grateful to F M F de Groot, C Brouder, V Briois and M A Arrio for fruitful discussions.

References

[1] Heintz J M, Drillon M, Kuentzler R, Dossmann Y, Kappler J P, Durmeyer O and Gautier F 1989 Z. *Phys.* B **76** 303
[2] Carley A F, Chalker P R, Riviere J C and Roberts M W 1987 *J. Chem. Soc. Faraday Trans.* **83** 351
[3] Beaurepaire E, Lewonczuk S, Ringeissen J, Parlebas J C, Uozumi T, Okada K and Kotani A 1993 *Europhys. Lett.* **22** 463
[4] Khan M A, Kotani A and Parlebas J C 1991 *J. Phys.: Condens. Matter* **3** 1763
[5] Soriano L, Abbate M, Fuggle J C, Jimenez M A, Sanz J M, Mythen C and Padmore H A 1993 *Solid State Commun.* **87** 699
[6] de Groot F M F, Figueiredo M O, Basto M J, Abbate M, Petersen H and Fuggle J C 1992 *Phys. Chem. Miner.* **19** 140
[7] Brydson R, Sauer H, Engel W, Thomas J M, Zeitler E, Kosugi N and Kuroda H 1989 *J. Phys.: Condens. Matter* **1** 797
[8] Brydson R, Williams B G, Engel W, Sauer H, Zeitler E and Thomas J M 1987 *Solid State Commun.* **64** 609
[9] Okada K and Kotani A 1993 *J. Electron. Spectrosc. Relat. Phenom.* **62** 131
[10] Crocombette J P and Jollet F 1994 *J. Phys.: Condens. Matter* **6** 8341
[11] Figgis B N 1966 *Introduction to Ligand Field* (New York: Interscience)
[12] Slater J C and Koster G F 1954 *Phys. Rev.* **94** 1498
[13] Harrison W A 1980 *Electronic Structure and the Properties of Solids* (San Francisco: Freeman)
[14] Griffith J S 1961 *The Theory of Transition Metal Ions* (Cambridge: Cambridge University Press)
[15] Fuggle J C and Inglesfield J E 1992 *Unoccupied Electronic States, Topics in Applied Physics* (Berlin: Springer) appendix B, p 347
[16] Moore C E 1971 *NBS Circular* 467
[17] de Groot F M F, Fuggle J C, Thole B T and Sawatzky G 1990 *Phys. Rev.* B **41** 928
[18] Cowan R D 1981 *The Theory of Atomic Structure and Spectra* (Berkeley, CA: University of California Press)
[19] Thole B T and van der Laan G 1988 *Phys. Rev.* B **38** 3158
[20] Parlebas J C 1992 *J. Physique* I **2** 1369
[21] König E and Kremer S 1977 *Ligand Field Energy Diagrams* (New York: Plenum)
[22] van Veenendaal M A and Sawatzky G A 1993 *Phys. Rev. Lett.* **70** 2459
[23] Liehr A D and Ballhausen C J 1958 *Ann. Phys.* **3** 304
[24] McClure D S 1962 *J. Chem. Phys.* **36** 2757
[25] Koswig H D, Retter U and Ulrici W 1967 *Phys. Status Solidi* **24** 605